Geology

Imaging the source region of Cascadia tremor and intermediate-depth earthquakes

Geoffrey A. Abers, Laura S. MacKenzie, Stéphane Rondenay, Zhu Zhang, Aaron G. Wech and Kenneth C. Creager

Geology 2009;37;1119-1122
doi: 10.1130/G30143A.1

Notes

Imaging the source region of Cascadia tremor and intermediate-depth earthquakes

Geoffrey A. Abers[1]*, Laura S. MacKenzie[2], Stéphane Rondenay[3], Zhu Zhang[4], Aaron G. Wech[5], and Kenneth C. Creager[5]
[1]Lamont-Doherty Earth Observatory of Columbia University, Route 9W, P.O. Box 1000, Palisades, New York 10964, USA
[2]Schlumberger Data and Consulting Services 6501 S. Fiddler's Green, Greenwood Village, Colorado 80111, USA
[3]Department of Earth, Atmospheric and Planetary Sciences, Massachusetts Institute of Technology, Cambridge, Massachusetts 02139, USA
[4]Department of Geology and Geophysics, University of Wyoming, Laramie, Wyoming 82070, USA
[5]Department of Earth and Space Science, University of Washington, Seattle, Washington 98195, USA

ABSTRACT

The subduction of hydrated oceanic crust releases volatiles that weaken the plate boundary interface, trigger earthquakes, and regulate transient phenomena such as episodic tremor and slip (ETS). It is not clear how dehydration can separately induce earthquakes within the subducting plate and ETS, partly because few data exist on their relationship to subduction zone structures. We present results of a seismic experiment in the Washington Cascades, United States, that images a region producing both earthquake types. Migration of scattered teleseismic waves provides images of low-velocity subducting crust at depths <40–45 km with sharp boundaries above and below it. The sharp upper boundary indicates a layer of weak sediment or an overpressured fault zone that terminates abruptly downdip at 40–45 km depth. Regular earthquakes are at the top of the mantle within the downgoing plate everywhere the plate is <95 km deep, but ETS only exists where the sharp upper boundary occurs. The ETS location supports models of slow slip that require near-lithostatic fluid pressure, whereas regular earthquakes nucleate closer to the origin of metamorphic dehydration. Very low shear stresses on the plate boundary may limit seismicity to ETS and similar phenomena.

INTRODUCTION

As oceanic plates subduct, gabbroic crust metamorphoses to anhydrous eclogite. This process releases mineral-bound H_2O and provides a fluid source at depth, which has been implicated in the generation of earthquakes (Green and Houston, 1995; Hacker et al., 2003), both regular intermediate-depth earthquakes (Kirby et al., 1996) and recently discovered slow earthquakes, including episodic tremor and slip (ETS) (Obara, 2002; Rogers and Dragert, 2003). However, the two types of earthquakes differ in several ways (Ide et al., 2007), so somehow conditions must differ between the regions that produce them.

In order to better understand the conditions in which these two earthquake types occur, we conducted a broadband seismic experiment in the Washington Cascades (Washington State, United States). ETS is well known in Cascadia, where slab temperatures are estimated to be among the hottest of any subduction zone (Oleskevich et al., 1999; van Keken et al., 2002), and therefore slab dehydration is expected to occur at relatively shallow depths. Migration of scattered teleseismic waves has provided images of subducting crust elsewhere in Cascadia (Rondenay et al., 2001; Nicholson et al., 2005), and has revealed a major dehydration event at 40–45 km depth, where seismic velocities indicate that gabbroic crust disappears; this transition happens at greater depths in other, colder subduction zones (Rondenay et al., 2008). The Washington transect analyzed here is one of the few parts of Cascadia showing both well-located ETS and intraslab earthquakes (i.e., earthquakes within the subducting plate; Kirby et al., 1996), including some of the deepest and largest recorded in Cascadia (Fig. 1), making direct comparisons possible. We see evidence for a very sharp and inverted velocity step that we interpret as the top to the subduction interface, probably reflecting weak subducting sediments or fluid overpressures. Regular earthquakes are just below the subducting Moho.

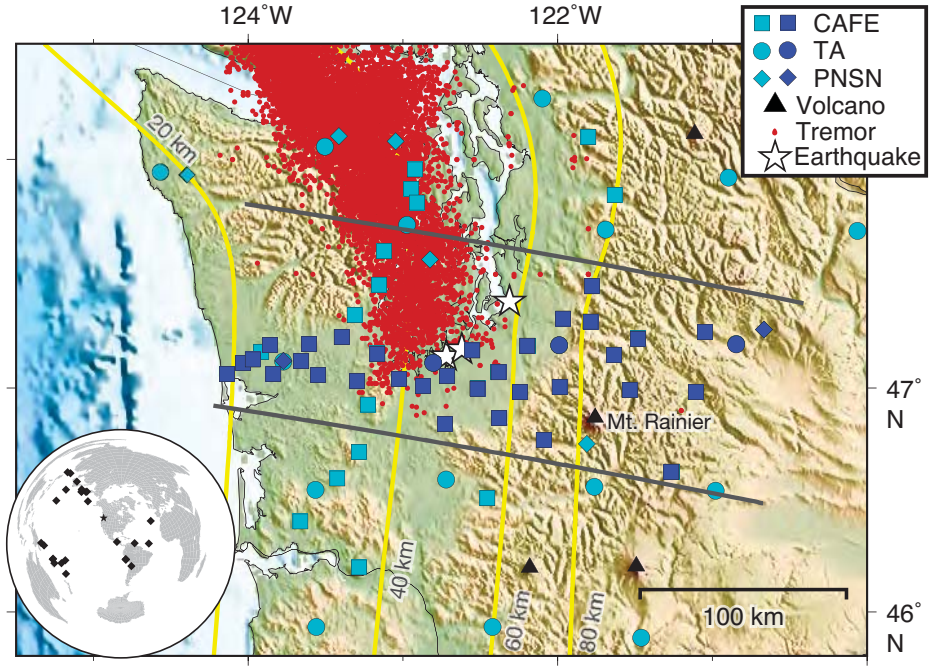

Figure 1. Broadband seismic stations used in this study (blue), tremor (red dots), and contours to slab seismicity (yellow). Stations symbols are dark blue if used in migration image or light blue if only used to estimate incident wavefield and for earthquake location. Symbol shape indicates network (legend): CAFE—Cascadia Arrays for Earthscope; TA—Earthscope Transportable Array; PNSN—Pacific Northwest Seismic Network. Tremors (dots) from 2004, 2005, 2007, and 2008 sequences located by automated detection technique (Wech and Creager, 2008). Contours show depth to Juan de Fuca slab at 20 km intervals (McCrory et al., 2004). Dark lines denote cross-section projection region (Fig. 2). Stars show epicenters of three largest (*M* > 6.5) recorded intraslab earthquakes, in 1949, 1965, and 2001(Data Repository, Section C; see footnote 1). Inset, lower left, shows earthquakes used in migration (diamonds).

*E-mail: abers@ldeo.columbia.edu.

DATA AND METHODS

The Cascadia Arrays For Earthscope (CAFE) experiment deployed 47 broadband seismometers from August 2006 to September 2008 (Fig. 1), supplemented by 32 additional broadband seismographs in the region (see the GSA Data Repository, Section A[1]). We show three analyses of the first 15 months of these data: migration of scattered teleseismic *P* coda, location of regular earthquakes, and location of tremor (Fig. 2). The scattered wavefield is extracted from the teleseismic *P* coda and migrated in a manner that estimates the *P* and *S* velocity variations (Bostock et al., 2001; Rondenay et al., 2005). Sharp gradients or discontinuities produce scattering, so the resulting images show the perturbations to the *S* velocity field, *dVs/Vs*, in a manner that highlights sharp boundaries such as that expected between gabbroic oceanic crust and surrounding peridotitic mantle (Fig. 2B). These data also allow construction of a rare image from *P*-to-*P* scattering that constrains variations in *P*-wave velocity, *dVp/Vp* (Fig. 2C). Although lower in resolution, as expected, the *P* image shows independent confirmation of the main structures. Migration has been repeated over a range of weighting schemes and projection azimuths to optimize the image, and within a series of one-dimensional velocity models (MacKenzie, 2008).

Earthquakes are relocated from arrival times determined at the same stations and in the same reference velocity models as those used for migration. Tremors are located using the same model and an automatic envelope correlation method (Wech and Creager, 2008). The relocated earthquakes have local magnitudes ranging from 1.1 to 3.2.

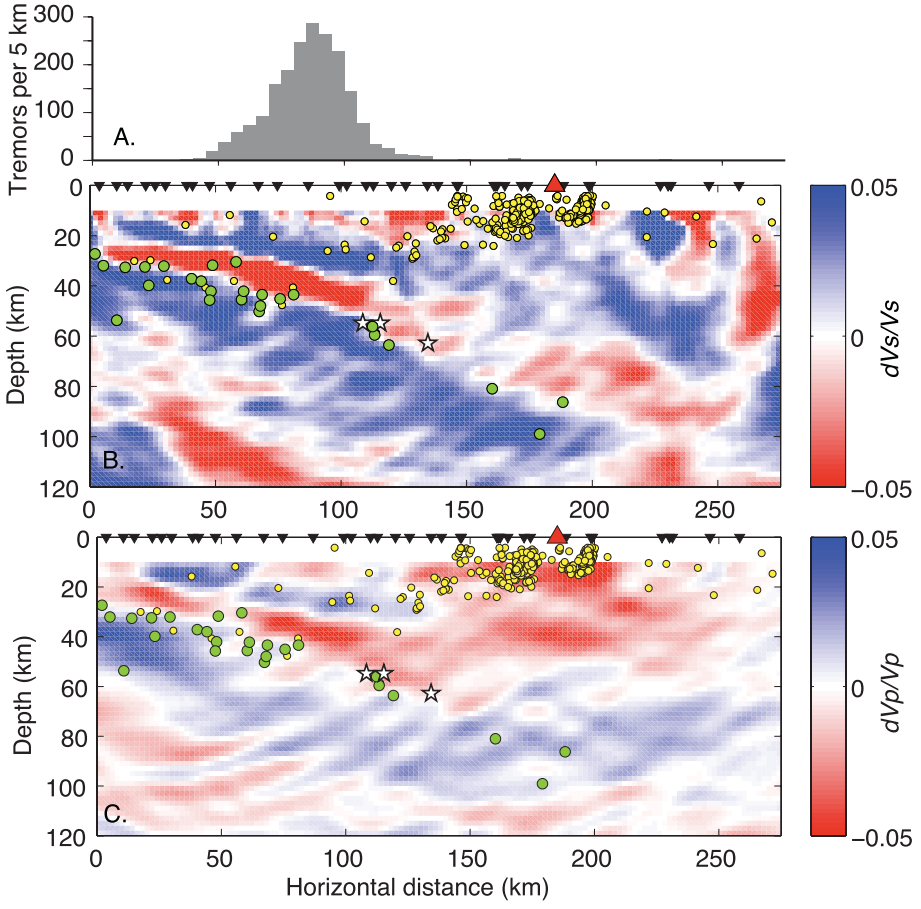

Figure 2. Migration images for central Washington, with seismicity and tremor. Transect location shown on Figure 1; horizontal distance of 0 km corresponds to coastline. A: Histogram of number of tremors shown in Figure 1 between section lines, in bins 5 km wide. B: *S*-wave velocity variations *dVs/Vs*, from migration. Green circles: earthquakes >20 km deep and between 47°N and 48°N latitude, occurring during CAFE and relocated using same velocity model as migration. Yellow circles: select events from local catalog (McCrory et al., 2004). Red triangle: Mt. Rainier volcano. Stars: three largest (*M* > 6.5) recorded earthquakes at waveform-derived depths. C: Same as B, but for *P*-wave velocity variations *dVp/Vp*.

IMAGE OF THE SUBDUCTING PLATE

A dipping low-velocity zone dominates the *S*-wave image at depths of 20–45 km and within 110 km of the coast, outlining the subducted crust of the Juan de Fuca plate (Fig. 2). This layer has a thickness of 5 km at the coast, thickening slightly landward, and rapidly becoming weaker at 40–45 km depth and 110 km from the coast, similar to images obtained previously in Cascadia with this method (Rondenay et al., 2001; Nicholson et al., 2005). This and other Cascadia images show similar velocity contrasts of 10%–15% between the low-velocity layer and its surroundings. The velocities and changes at 40–45 km depth indicate that the principal conversion from basaltic crust to eclogite takes place near this depth (Bostock et al., 2002; Hacker et al., 2003; Rondenay et al., 2008). The noisier *P*-wave image (Fig. 2C) shows similar features, but the sharp change at 40–45 km depth is less obvious. Unlike images from Vancouver (Nicholson et al., 2005) and Oregon (Rondenay et al., 2001; Bostock et al., 2002), the upper plate Moho is faint, a complication that is the subject of an ongoing study.

It is not clear why the low-velocity layer should show strong velocity contrasts at both its top and bottom boundaries at <45 km depth. The bottom boundary is explained as oceanic Moho; however, the overlying Cascadia forearc crust is likely composed of mafic rocks of an Eocene accreted terrane (Parsons et al., 1999), similar in bulk composition and seismic velocities to the subducting oceanic crust. Velocities probably increase rapidly with depth in the low-velocity layer, so that velocities in its uppermost part are much lower than those of overlying anhydrous gabbros. Stacks of observed receiver functions (the signals used to generate the migration images) resemble predictions calculated both for a simple low-velocity channel and for a channel with steep vertical gradient (Fig. 3), but only the latter model allows both strong conversions and plausible velocities outside the low-velocity layer (Data Repository, Section D).

Perhaps low velocities at the top of the low-velocity layer represent metamorphosed subducted sediment. A sedimentary layer at least 3 km thick blankets the Juan de Fuca plate offshore at the trench (Flueh et al., 1998), an unknown fraction of which bypasses the accretionary prism and would be just below the plate boundary. Metamorphosed sediments should have significantly slower seismic velocities than gabbros. Alternatively, or in addition, velocities at the top of the plate could be reduced by fluids in overpressured channels within or immediately below the plate interface (Audet et al., 2009). Elevated fluid pressures would arise from dehydration-produced

[1]GSA Data Repository item 2009277, Table DR1 (one-dimensional velocity model used for migration and hypocenters), and Figures DR1–DR4, is available online at www.geosociety.org/pubs/ft2009.htm, or on request from editing@geosociety.org or Documents Secretary, GSA, P.O. Box 9140, Boulder, CO 80301, USA.

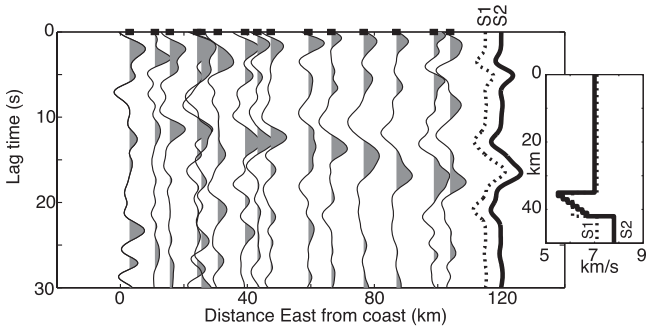

Figure 3. Single-station receiver functions and simple models for stations <100 km from coast. Thin lines: radial-component signals stacked over events at back-azimuths west of array (180°–360°), plotted by distance from coastline. Signals subjected to 0.3 Hz low-pass Gaussian filters. Traces marked S1 and S2 are predictions for two models of low-velocity zone illustrated in inset; dotted line corresponds to simple low-velocity channel, and thick line has velocity gradient within layer to mimic sediments or free fluids at top of subducting crust. *Vp/Vs* = 1.80 for case S1, and increases to 1.90–2.00 at top of case S2.

fluids migrating upward, encountering permeability barriers along the thrust zone.

To test these possibilities, the signals shown in Figure 3 are analyzed in detail and compared with predictions for candidate materials (Data Repository, Sections E, F, and G). If the low-velocity zone is divided in two, and the lower layer resembles oceanic crust (7 km thick, *P* velocity *Vp* = 6.3–7.2 km/s), then the best-fit upper layer is 2.5–5.5 km thick with *Vp* = 5.0 ± 0.3 km/s. These velocities are somewhat lower than expected for terrigenous metasediments, for which *Vp* averages 5.4–6.5 km/s, but prediction uncertainties and anisotropy effects in highly foliated mica schists can be large. Still, *Vp* of 5.0 km/s and high *Vp/Vs* ratios probably require some fluids to be present at high pressures to sustain porosity. Less porosity would be needed to match observed velocities for a metasediment-dominated fault zone than a mafic or ultramafic one; the relationship depends heavily upon pore geometry. Regardless, no major reactions happen within metasediments at 40–45 km depth (Hacker, 2008), so another process must change the velocity structure, indicating the importance of fluids. Perhaps a permeability seal to the overpressured fault zone is disrupted here (Audet et al., 2009).

The base of the low-velocity layer, probably the oceanic Moho, continues coherently to 80–90 km depth as a weak (4%–5%) discontinuity in *dVs/Vs* and to 65 km depth in *dVp/Vp*. Anhydrous eclogite has seismic velocities indistinguishable from peridotite, so a discontinuity would not be expected once oceanic crust has fully eclogitized (Abers et al., 2006; Hacker et al., 2003). The persistence of Moho suggests that the crust does not fully convert until 80–90 km depth here, although probably major garnet-forming reactions occur shallower. For example, coarse-grained gabbro may persist metastably where fluids are not available to catalyze reactions, and weakly hydrated assemblages such as zoisite-amphibole eclogite may be stable in mafic rocks at this depth range and would have appropriate seismic velocities (Hacker et al., 2003). Thus, the velocity step at 45–90 km depth is probably a consequence of metamorphic processes rather than fluid pressures.

ETS AND DEHYDRATION

ETS has been well documented in northern Cascadia (Rogers and Dragert, 2003; Wech and Creager, 2008), the main zone extending south to 47°N (Fig. 1). Although tremor in Cascadia has been located at a wide range of depths using methods that rely upon waveform envelopes (Kao et al., 2005), additional constraints from *S* minus *P* times indicate that Cascadia tremor comes from at or very near the plate interface (La Rocca et al., 2009). There is some dispute about the location of the plate interface, a zone of high reflectivity 10–20 km above intraslab seismicity (the E reflector), that has been interpreted as part of a shallower, thick plate boundary beneath Vancouver Island (e.g., Calvert et al., 2006). Still, geodetic inversions (Rogers and Dragert, 2003) demonstrate that slow slip events in Cascadia are collocated in space and time with tremor and are on the plate interface, as do locations of low-frequency earthquakes in southern Japan (Shelly et al., 2006), so it is reasonable to assume that the structure of the plate interface region controls the occurrence of ETS.

Tremor occurs only where subducted crust appears as a strong low-velocity channel (Fig. 2). The downdip end of the tremor corresponds within 5 km to the downdip end of the strong low-velocity crustal anomaly, 110 km from the coast (Fig. 2). Comparison with the imaging shows that tremor is localized to the region where the plate boundary is inferred to be a zone of overpressured dehydration-produced fluids. A similar conclusion has been proposed for northern Cascadia (Audet et al., 2009), and a region of low velocities and elevated Poisson's ratio is along the Nankai plate boundary where tremor has been observed (Kodaira et al., 2004), also indicating elevated fluid pressure. High fluid pressures may be a prerequisite for non-volcanic tremor; for example, dynamic friction models can produce episodic slip at observed periodicities if near-lithostatic pressures are present (Liu and Rice, 2007; Rubin, 2008).

REGULAR INTRASLAB EARTHQUAKES

The Washington transect also includes abundant regular intraslab earthquakes. The deepest earthquakes anywhere in the Cascades are near 95 km depth north of the Mount Rainier volcano, and the three largest recorded intraslab earthquakes in Cascadia (magnitude 6.5–7) occurred within the transect and are within a few kilometers of the downdip termination of the low-velocity layer and tremor (Fig. 2). Here and elsewhere along the profile, virtually all earthquakes are within a few kilometers of the Moho of the downgoing plate. Tests conducted by varying the *P* and *S* velocity models for both migration and earthquake location show that this relationship is robust (Data Repository, Section H; MacKenzie, 2008). This result is somewhat similar to those seen previously in this region, where the earthquakes are below the subducting Moho where it is <50 km deep and above it at greater depth (Nicholson et al., 2005; Preston et al., 2003), although here the deeper earthquakes still appear to be at or below the Moho. The pattern in southern Japan is similar (e.g., Shelly et al., 2006), although other, colder subduction zones show intraslab seismicity within subducted crust (e.g., Abers et al., 2006; Nakajima et al., 2001).

EARTHQUAKES AND DEHYDRATION

The Juan de Fuca plate is young, ca. 10 Ma at the trench (Wilson, 2002), and subducts slowly, <30 mm/yr in the downdip direction (McCaffrey et al., 2007), making temperatures within the subducted crust among the hottest of any subduction zone (Rondenay et al., 2008). Temperatures likely exceed the breakdown of most hydrous phases stable beyond 1.5 GPa (45 km depth) within mafic rocks, although thermal models permit a thin (<5 km wide) region just below the Moho, where hydrated, chlorite- and potentially serpentine-bearing peridotite would be present (Hacker et al., 2003). As the uppermost oceanic mantle dehydrates, critical reactions take place immediately below the subducting Moho, and these may trigger earthquakes. However, the relationship between intraslab seismicity and fluids seems complex, since regular earthquakes do not occur at the plate interface where we infer high porosity and high fluid pressures. This implies that reduction in effective normal stress alone does not trigger regular intraslab earthquakes, and in fact, very low sustained shear stress may be insufficient to drive them. Rather, some other aspect of the dehydration process must regulate earthquakes, as indicated by recent laboratory experiments that demonstrate the occurrence of faulting at the sites of dehydration even when volumes

decrease during reaction, so overpressure would not be expected over large volumes (Jung et al., 2004). Further experiments are needed to better understand these processes.

CONCLUSIONS

In summary, ETS and intraslab earthquakes occur near each other and seemingly associated with dehydration of subducting plates, but in distinctly different parts of the system. Unlike intraslab earthquakes, ETS occurs in a large, continuous fault zone where overpressured conditions are inferred, and where possibly high mechanical and permeability anisotropy may be present due to fault zone structure and rock fabrics. By contrast, intraslab dehydration does not obviously occur on well-established faults, but occurs where dehydration may be acting to lubricate or embrittle otherwise strong material, allowing large shear stresses to drive intraslab earthquakes.

ACKNOWLEDGMENTS

The Cascadia Arrays For Earthscope experiment (CAFE) is an EarthScope Flexible Array program, supported by the Incorporated Research Institutions for Seismology (IRIS) Program for Array Seismic Studies of the Continental Lithosphere (PASSCAL) Instrument Center. We thank the large group of volunteers who participated in CAFE operations, B. Hacker for perspectives on metasediments, and M. Bostock and an anonymous reviewer for constructive reviews. Additional support and data were provided by the Pacific Northwest Seismic Center. This work was funded by National Science Foundation grants EAR-0544847 (Boston University/Lamont-Doherty Earth Observatory) and EAR-0544996 (Massachusetts Institute of Technology).

REFERENCES CITED

Abers, G.A., van Keken, P.E., Kneller, E.A., Ferris, A., and Stachnik, J.C., 2006, The thermal structure of subduction zones constrained by seismic imaging: Implications for slab dehydration and wedge flow: Earth and Planetary Science Letters, v. 241, p. 387–397, doi: 10.1016/j.epsl.2005.11.055.

Audet, P., Bostock, M.G., Christensen, N.I., and Peacock, S.M., 2009, Seismic evidence for overpressured subducted oceanic crust and sealing of the megathrust: Nature, v. 457, p. 76–78, doi: 10.1038/nature07650.

Bostock, M.G., Rondenay, S., and Shragge, J., 2001, Multiparameter two-dimensional inversion of scattered teleseismic body waves; 1, Theory for oblique incidence: Journal of Geophysical Research, v. 106, p. 30,771–30,782, doi: 10.1029/2001JB000330.

Bostock, M.G., Hyndman, R.D., Rondenay, S., and Peacock, S.M., 2002, An inverted continental Moho and serpentinization of the forearc mantle: Nature, v. 417, p. 536–538, doi: 10.1038/417536a.

Calvert, A., Ramachandran, K., Kao, H., and Fisher, M.A., 2006, Local thickening of the Cascadia forearc crust and the origin of seismic reflectors in the uppermost mantle: Tectonophysics, v. 420, p. 175–188.

Flueh, E.R., Fisher, M.A., Bialas, J., Childs, J.R., Klaeschen, D., Kukowski, N., Parsons, T., Scholl, D.W., ten Brink, U., Trehu, A.M., and Vidal, N., 1998, New seismic images of the Cascadia subduction zone from SO108-ORWELL: Tectonophysics, v. 293, p. 69–84, doi: 10.1016/S0040-1951(98)00091-2.

Green, H.W., and Houston, H., 1995, The mechanics of deep earthquakes: Annual Review of Earth and Planetary Sciences, v. 23, p. 169–213, doi: 10.1146/annurev.ea.23.050195.001125.

Hacker, B.R., 2008, H_2O subduction beyond arcs: Geochemistry, Geophysics, Geosystems (G3), v. 9, Q03001, doi: 10.1029/2007GC001707.

Hacker, B.R., Peacock, S.M., Abers, G.A., and Holloway, S.D., 2003, Subduction factory 2. Are intermediate-depth earthquakes in subducting slabs linked to metamorphic dehydration reactions?: Journal of Geophysical Research, v. 108, 2030, doi: 10.1029/2001JB001129.

Ide, S., Beroza, G., Shelly, D.R., and Uchide, T., 2007, A scaling law for slow earthquakes: Nature, v. 447, p. 76–79, doi: 10.1038/nature05780.

Jung, H., Green, H.W., and Dobrzhinetskaya, L.F., 2004, Intermediate-depth earthquake faulting by dehydration embrittlement with negative volume change: Nature, v. 428, p. 545–549, doi: 10.1038/nature02412.

Kao, H., Shan, S.-J., Dragert, H., Rogers, G., Cassidy, J.F., and Ramachandran, K., 2005, A wide depth distribution of seismic tremors along the northern Cascadia margin: Nature, v. 436, p. 841–844, doi: 10.1038/nature03903.

Kirby, S., Engdahl, E.R., and Denlinger, R., 1996, Intermediate-depth intraslab earthquakes and arc volcanism as physical expressions of crustal and uppermost mantle metamorphism in subducting slabs, *in* Bebout, G.E., et al., eds., Subduction: Top to bottom: American Geophysical Union Geophysical Monograph 96, p. 195–214.

Kodaira, S., Iidaka, T., Kato, A., Park, J.-O., Iwasaki, T., and Kaneda, Y., 2004, High pore fluid pressure may cause silent slip in the Nankai Trough: Science, v. 304, p. 1295–1298, doi: 10.1126/science.1096535.

La Rocca, M., Creager, K.C., Galluzzo, D., Malone, S., Vidale, J.E., Sweet, J.R., and Wech, A.G., 2009, Cascadia tremor located near plate interface constrained by *S* minus *P* wave times: Science, v. 323, p. 620–623, doi: 10.1126/science.1167112.

Liu, Y.J., and Rice, J.R., 2007, Spontaneous and triggered aseismic deformation transients in a subduction fault model: Journal of Geophysical Research, v. 112, B09404, doi: 10.1029/2007JB004930.

MacKenzie, L.S., 2008, A receiver function study of the Central America and Cascadia subduction zone systems [Ph.D. thesis]:Boston, Massachusetts, Boston University, 163 p.

McCaffrey, R., Qamar, A.I., King, R.W., Wells, R., Khazaradze, G., Williams, C.A., Stevens, C.W., Vollick, J.J., and Zwick, P.C., 2007, Fault locking, block rotation and crustal deformation in the Pacific Northwest: Geophysical Journal International, v. 169, p. 1315–1340, doi: 10.1111/j.1365-246X.2007.03371.x.

McCrory, P.A., Blair, J.L., Oppenheimer, D.H., and Walter, S.R., 2004, Depth to the Juan de Fuca slab beneath the Cascadia subduction margin—A 3-D model for sorting earthquakes: U.S. Geological Survey Data Series, v. 91, version 1.2, http://pubs.usgs.gov/ds/91/.

Nakajima, J., Matsuzawa, T., Hasegawa, A., and Zhao, D., 2001, Three-dimensional structure of *Vp, Vs,* and *Vp/Vs* beneath northeastern Japan: Implications for arc magmatism and fluids: Journal of Geophysical Research, v. 106, p. 21,843–21,857, doi: 10.1029/2000JB000008.

Nicholson, T., Bostock, M., and Cassidy, J.F., 2005, New constraints on subduction zone structure in northern Cascadia: Geophysical Journal International, v. 151, p. 849–859, doi: 10.1111/j.1365-246X.2005.02605.x.

Obara, K., 2002, Nonvolcanic deep tremor associated with subduction in southwest Japan: Science, v. 296, p. 1679–1681, doi: 10.1126/science.1070378.

Oleskevich, D., Hyndman, R., and Wang, K., 1999, The updip and downdip limits to great subduction earthquakes: Thermal and structural models of Cascadia, south Alaska, SW Japan, and Chile: Journal of Geophysical Research, v. 104, p. 14,965–14,991, doi: 10.1029/1999JB900060.

Parsons, T., Wells, R.E., Fisher, M.A., Flueh, E., and ten Brink, U.S., 1999, Three-dimensional velocity structure of Siletzia and other accreted terranes in the Cascadia forearc of Washington: Journal of Geophysical Research, v. 104, p. 18,015–18,039, doi: 10.1029/1999JB900106.

Preston, L.A., Creager, K.C., Crosson, R.S., Brocher, T.M., and Trehu, A.M., 2003, Intraslab earthquakes: Dehydration of the Cascadia slab: Science, v. 302, p. 1197–1200, doi: 10.1126/science.1090751.

Rogers, G., and Dragert, H., 2003, Episodic tremor and slip on the Cascadia subduction zone: The chatter of silent slip: Science, v. 300, p. 1942–1943, doi: 10.1126/science.1084783.

Rondenay, S., Bostock, M.G., and Shragge, J., 2001, Multiparameter two-dimensional inversion of scattered teleseismic body waves, 3, Application to the Cascadia 1993 data set: Journal of Geophysical Research, v. 106, p. 30,795–30,808, doi: 10.1029/2000JB000039.

Rondenay, S., Bostock, M.G., and Fischer, K.M., 2005, Multichannel inversion of scattered teleseismic body waves: Practical considerations and applicability, *in* Levander, A., and Nolet, G., eds., Seismic Earth: Array analysis of broadband seismograms: American Geophysical Union Geophysical Monograph 157, p. 187–203.

Rondenay, S., Abers, G.A., and van Keken, P.E., 2008, Seismic imaging of subduction zone metamorphism: Geology, v. 36, p. 275–278, doi: 10.1130/G24112A.1.

Rubin, A.M., 2008, Episodic slow slip events and rate-and-state friction: Journal of Geophysical Research, v. 113, B11414, doi: 10.1029/2008JB005642.

Shelly, D.R., Beroza, G.C., Zhang, H., Thurber, C.H., and Ide, S., 2006, High-resolution subduction zone seismicity and velocity structure beneath Ibaraki Prefecture, Japan: Journal of Geophysical Research, v. 111, B06311, doi: 10.1029/2005JB004081.

van Keken, P.E., Kiefer, B., and Peacock, S.M., 2002, High-resolution models of subduction zones: Implications for mineral dehydration reactions and the transport of water into the deep mantle: Geochemistry, Geophysics, Geosystems, v. 3, p. 1056.

Wech, A.G., and Creager, K.C., 2008, Automated detection and location of Cascadia tremor: Geophysical Research Letters, v. 35, L20302, doi: 10.1029/2008GL035458.

Wilson, D.S., 2002, The Juan de Fuca plate and slab: Isochron structure and Cenozoic plate motions, in Kirby, S., et al., eds., The Cascadia subduction zone and related subduction systems seismic structure, intraslab earthquakes and processes, and earthquake hazards: U.S. Geological Survey Open-File Report 02-328, p. 9–12.

Manuscript received 16 February 2009
Revised manuscript received 17 July 2009
Manuscript accepted 21 July 2009

Printed in USA